

# Mechanism of ubiquitylation by dimeric RING ligase RNF4

Anna Plechanovová<sup>1</sup>, Ellis G Jaffray<sup>1</sup>, Stephen A McMahon<sup>2</sup>, Kenneth A Johnson<sup>2</sup>, Iva Navrátilová<sup>3</sup>, James H Naismith<sup>2</sup> & Ronald T Hay<sup>1</sup>

Mammalian RNF4 is a dimeric RING ubiquitin E3 ligase that ubiquitylates poly-SUMOylated proteins. We found that RNF4 bound ubiquitin-charged UbcH5a tightly but free UbcH5a weakly. To provide insight into the mechanism of RING-mediated ubiquitylation, we docked the UbcH5~ubiquitin thioester onto the RNF4 RING structure. This revealed that with E2 bound to one monomer of RNF4, the thioester-linked ubiquitin could reach across the dimer to engage the other monomer. In this model, the 'Ile44 hydrophobic patch' of ubiquitin is predicted to engage a conserved tyrosine located at the dimer interface of the RING, and mutation of these residues blocked ubiquitylation activity. Thus, dimeric RING ligases are not simply inert scaffolds that bring substrate and E2-loaded ubiquitin into close proximity. Instead, they facilitate ubiquitin transfer by preferentially binding the E2~ubiquitin thioester across the dimer and activating the thioester bond for catalysis.

Ubiquitin conjugation is a widely used and highly flexible means of altering the fate of target proteins. Ubiquitin is first activated by formation of a thioester bond between its C terminus and a cysteine residue of the E1 activating enzyme. It is then transferred to an E2 conjugating enzyme, again forming a thioester bond with the active site cysteine residue. Ubiquitin transfer is accomplished when the  $\epsilon$ -amino group of a lysine side chain in the target protein attacks the thioester, yielding an isopeptide bond. This final step is usually catalyzed by a ubiquitin E3 ligase that recruits both the E2~ubiquitin (E2~Ub) thioester and the specific substrate<sup>1,2</sup>. There are two broad classes of ubiquitin E3 ligases: 'homologous to E6-AP C terminus' (HECT) ligases and 'really interesting new gene' (RING) ligases<sup>3</sup>. HECT-type ubiquitin E3 ligases contain a catalytic cysteine residue that forms a thioester intermediate with ubiquitin before the final transfer<sup>1</sup>. RING E3 ligases do not form a covalent intermediate, but catalyze direct transfer of ubiquitin from the E2~Ub thioester to a substrate. RING proteins contain a conserved arrangement of cysteine and histidine residues that coordinate two zinc atoms and cross-brace the folded structure.

Like ubiquitin, small ubiquitin-like modifier (SUMO) functions as a post-translational modification of other proteins<sup>4</sup>. SUMO-targeted ubiquitin ligases (STUbLs) are a conserved family of proteins that target SUMO-modified proteins for ubiquitylation<sup>5–10</sup>, as typified by RING finger protein 4 (RNF4) in mammals<sup>11–13</sup>. STUbLs contain multiple SUMO-interaction motifs (SIMs)<sup>14–16</sup> and a RING domain, allowing them to specifically recognize poly-SUMO chains. In response to arsenic therapy, the promyelocytic leukemia protein (PML) is modified with a poly-SUMO chain that recruits RNF4, thus targeting the modified protein for ubiquitin-mediated degradation<sup>12,13</sup>.

To determine the mechanism of RING-mediated ubiquitylation, we first obtained the structure of the homodimeric RNF4 RING domain from *Rattus norvegicus*. To probe the role of dimerization in RING function, we docked E2~Ub thioester onto the experimental structure of the RNF4 RING domain. The model shows the E2 bound to one monomer, while the thioester-linked ubiquitin engages the other monomer, potentially explaining the requirement for the dimer. The predicted interface between ubiquitin and RNF4 centers on the 'Ile44 hydrophobic patch' of ubiquitin and the conserved Tyr193 of the RNF4 RING. Mutation of these residues abolished the preferential interaction between the RING domain and ubiquitin-loaded E2, and abrogated ubiquitin E3 ligase activity. Thus, dimeric RING ligases such as RNF4 do not act as an inert scaffold, but mediate catalysis by binding E2~Ub thioester, activating the thioester bond and thus allowing efficient transfer of ubiquitin to substrate.

## RESULTS

### RNF4 RING domain is sufficient for ubiquitylation activity

RNF4 has a C-terminal RING domain required for ubiquitin E3 ligase activity<sup>13</sup>, while four tandem SIMs located in the N-terminal region provide specificity for binding to its substrate, poly-SUMO chains (Supplementary Fig. 1a,b). In the absence of substrate, RNF4 attaches ubiquitin to its internal lysine residues (autoubiquitylation). The isolated RING domain of RNF4 was active in autoubiquitylation, confirming that the RING domain is sufficient for ubiquitin transfer (Supplementary Fig. 1c). However, it was unable to ubiquitylate poly-SUMO-2 chains (Supplementary Fig. 1d). We generated a linear head-to-tail fusion of four SUMO-2 molecules (termed 4× SUMO-2) as a model substrate for RNF4, as longer poly-SUMO chains ( $N \geq 4$ )

<sup>1</sup>Wellcome Trust Centre for Gene Regulation and Expression, College of Life Sciences, University of Dundee, Dundee, UK. <sup>2</sup>Biomedical Sciences Research Complex, University of St. Andrews, St. Andrews, UK. <sup>3</sup>Division of Biological Chemistry and Drug Discovery, College of Life Sciences, University of Dundee, Dundee, UK. Correspondence should be addressed to R.T.H. (r.t.hay@dundee.ac.uk).

Received 19 May 2010; accepted 24 June 2011; published online 21 August 2011; doi:10.1038/nsmb.2108

are efficiently ubiquitylated by RNF4 (ref. 13). 4×SUMO-2 underwent RNF4-dependent ubiquitylation with similar efficiency to that of isopeptide bond-linked SUMO-2 tetramers (**Supplementary Fig. 2**).

To study the mechanism of RNF4-mediated ubiquitylation, we established a single-turnover substrate-ubiquitylation assay in which E2 (UbcH5a) was first charged with ubiquitin in the absence of substrate and E3. ATP was then depleted by the addition of apyrase to stop further E1-mediated loading of E2. Subsequently, RNF4 and substrate were added to initiate transfer of ubiquitin from E2 to substrate.  $^{125}\text{I}$ -labeled 4×SUMO-2 was efficiently ubiquitylated by RNF4 (**Fig. 1a,b**). Moreover, with the two substrates (4×SUMO-2 and E2~Ub) in excess, the reaction rate was linearly dependent on the concentration of RNF4 (for example, see **Fig. 2e**).

### RNF4 residues required for dimerization and E2 binding

As a first step in understanding RNF4-catalyzed ubiquitylation, we determined a 1.5-Å-resolution crystal structure of the RING domain of RNF4 (**Table 1** and **Supplementary Fig. 3**), which adopts a typical RING fold stabilized by two zinc ions coordinated by one histidine and seven cysteine residues. The RING domain crystallized in space group  $P4_132$  with one monomer in the asymmetric unit, but was dimeric in solution (**Supplementary Fig. 4**). In the crystal, the two subunits of a dimer are related by a crystallographic two-fold axis (**Fig. 1c**). This is consistent with a recently published structure for the RNF4 RING domain<sup>17</sup>.

The dimer interface is formed mainly by residues from the three  $\beta$ -strands, together with residues at the very end of the C terminus of RNF4 (**Fig. 1d**). In total, dimerization buries 518 Å<sup>2</sup> of

surface-accessible area of a monomer. The aromatic ring of Tyr193 appears to shield the dimer interface, while a hydrogen bond between the amide nitrogen of Tyr193 and the carbonyl oxygen of Gly159 in the other subunit bridges the two monomers. Mutation of residues at the dimer interface (Val161, His190, Ile192, Tyr193 and Ile194; **Fig. 1d**) disrupted dimerization (**Supplementary Fig. 5**). Monomeric RNF4 mutants were inactive, and only at ten times higher RNF4 concentration was limited substrate ubiquitylation detected (**Fig. 1e**).

RNF4 has a mode of dimerization similar to that of the RING domains of cIAP2 (ref. 18), MDM2-MDMX<sup>19</sup>, and the U-box domain of Prp19 (ref. 20). The structure of cIAP2 has also been solved in complex with E2 enzyme UbcH5b<sup>18</sup>. As RNF4 is active with the UbcH5 family of E2s<sup>13</sup> and several E2-interacting residues are conserved between cIAP2 and RNF4, we used the cIAP2-UbcH5b structure to model the interaction between RNF4 and UbcH5b (**Fig. 1f**). To verify the model, we changed putative E2-interacting residues to alanine in full-length RNF4 (**Fig. 1f**). With the exception of RNF4 I138A, the mutant proteins were correctly folded (**Supplementary Fig. 5**). Compared with wild-type RNF4, all mutations of putative E2-interacting residues reduced substrate-ubiquitylation activity of RNF4, and a double mutant, M140A R181A, showed no detectable E3 ligase activity (**Fig. 1g**).

To assess dimerization, we used fluorescence resonance energy transfer (FRET). When enhanced cyan fluorescent protein (ECFP)-tagged RNF4 was mixed with yellow fluorescent protein (YFP)-tagged RING domain, a FRET signal was detected that leveled off within the first 20 s (**Fig. 1h**). FRET was not observed when either YFP alone or dimerization-defective mutant YFP-RING I194A was added to ECFP-RNF4. A mutant with a disrupted E2-binding site (RING M140A R181A)

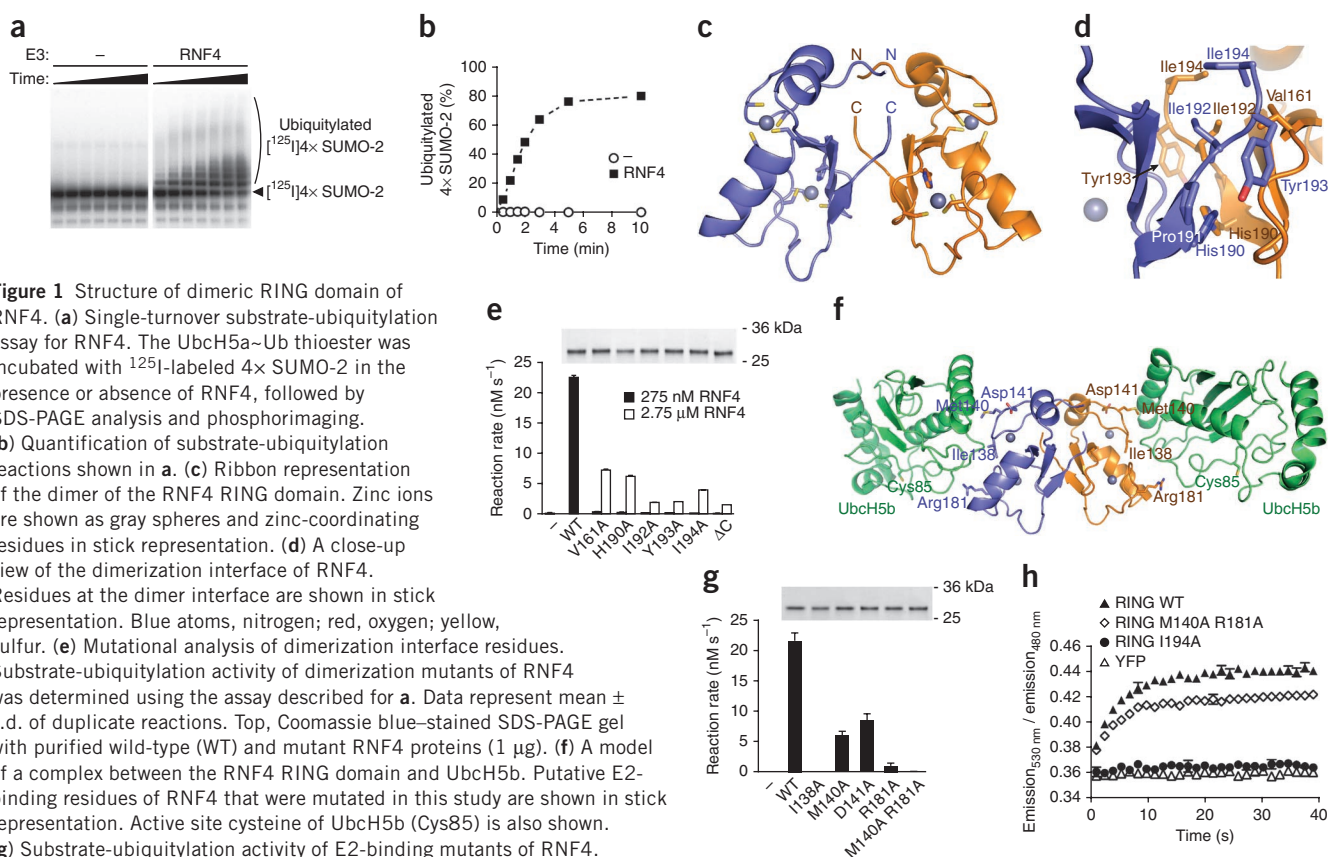


**Figure 1** Structure of dimeric RING domain of RNF4. **(a)** Single-turnover substrate-ubiquitylation assay for RNF4. The UbcH5a~Ub thioester was incubated with  $^{125}\text{I}$ -labeled 4×SUMO-2 in the presence or absence of RNF4, followed by SDS-PAGE analysis and phosphorimaging. **(b)** Quantification of substrate-ubiquitylation reactions shown in **a**. **(c)** Ribbon representation of the dimer of the RNF4 RING domain. Zinc ions are shown as gray spheres and zinc-coordinating residues in stick representation. **(d)** A close-up view of the dimerization interface of RNF4. Residues at the dimer interface are shown in stick representation. Blue atoms, nitrogen; red, oxygen; yellow, sulfur. **(e)** Mutational analysis of dimerization interface residues. Substrate-ubiquitylation activity of dimerization mutants of RNF4 was determined using the assay described for **a**. Data represent mean  $\pm$  s.d. of duplicate reactions. Top, Coomassie blue-stained SDS-PAGE gel with purified wild-type (WT) and mutant RNF4 proteins (1  $\mu\text{g}$ ). **(f)** A model of a complex between the RNF4 RING domain and UbcH5b. Putative E2-binding residues of RNF4 that were mutated in this study are shown in stick representation. Active site cysteine of UbcH5b (Cys85) is also shown. **(g)** Substrate-ubiquitylation activity of E2-binding mutants of RNF4. **(h)** A FRET-based *in vitro* assay to study dimerization of RNF4. ECFP-RNF4 (wild-type) was mixed with YFP or YFP-RING domain of RNF4 (wild-type or mutant) and FRET signal was measured. Data points represent mean  $\pm$  s.d. of triplicate measurements.

showed a similar but slightly reduced FRET signal. Thus, full-length RNF4 can form 'heterodimers' with the isolated RING domain. The rapid equilibration suggests that individual RNF4 molecules dynamically exchange between dimeric and monomeric states.

### Ubiquitylation by RNF4 can proceed *in cis* and *in trans*

Dimerization is essential for ubiquitin E3 ligase activity of RNF4 and other dimeric RING domain E3s<sup>18,19,21</sup>. However, monomeric RNF4 is capable of binding both substrate and E2. This poses a question: why is dimerization crucial? We hypothesized that ubiquitylation would proceed *in trans*, with E2 bound to one RING monomer and substrate bound to the other. To test this, we combined mutant RNF4 with disrupted E2-binding site (RNF4 M140A R181A) and isolated RING domain of wild-type RNF4 (RING WT). Inactive RNF4 M140A R181A has a substrate-binding site but does not interact with E2, whereas the isolated RING domain interacts with E2 but lacks a substrate-binding site. These proteins form heterodimers (Fig. 1h) that contain one substrate and one E2-binding site, located in different monomers; therefore, ubiquitylation can proceed only *in trans*. When both RNF4 M140A R181A and RING WT were mixed, substantial substrate ubiquitylation was observed, whereas neither protein alone could efficiently ubiquitylate substrate (Fig. 2a,b). Substrate-ubiquitylation activity of dimerization-deficient RNF4 I194A was not rescued by addition of RING WT, confirming that a functional dimer is required for ubiquitylation activity of RNF4.

Ubiquitylation by RNF4 can proceed *in trans*, but is this an obligate requirement, or can the reaction also proceed *in cis*? To address this question, we titrated the RING domain with disrupted E2-binding site (RING M140A R181A) into a substrate-ubiquitylation reaction containing full-length wild-type RNF4 (RNF4 WT). If ubiquitylation by RNF4 must proceed *in trans*, then heterodimers of RNF4 WT

and RING M140A R181A should not have substrate-ubiquitylation activity. Therefore, addition of an excess of RING M140A R181A to wild-type RNF4 should result in inhibition of E3 ligase activity (Fig. 2c). However, addition of up to a 200-fold molar excess of RING M140A R181A led to an increase in substrate-ubiquitylation activity of wild-type RNF4, rather than a decrease (Fig. 2d). Under the conditions used, substrate-ubiquitylation activity was proportional to concentration of RNF4 in the reaction (Fig. 2e). As expected, RING M140A R181A efficiently formed dimers with full-length RNF4 (Supplementary Fig. 6). As the heterodimer (RNF4 WT-RING M140A R181A) is active, this suggests that ubiquitylation can proceed *in cis*. Thus, RNF4-mediated ubiquitylation can proceed both *in cis* and *in trans*, implying that dimerization, although required for ubiquitylation activity, does not impose or create a particular spatial orientation of substrate- and E2-binding sites.

### RNF4 preferentially binds and activates ubiquitin-loaded E2

To gain insight into the mechanism of RING-catalyzed ubiquitylation, it would be desirable to interrogate a complex between the RING domain of RNF4 and UbCH5~Ub thioester. However, in the presence of RNF4, ubiquitin undergoes rapid transfer from E2 to lysine residues on the E3 in an autoubiquitylation reaction, precluding direct study. We thus changed the active site cysteine of UbCH5a to serine so that a more stable E2~Ub oxyester could be formed. In the absence of an E3, the UbCH5a C85S~Ub oxyester was stable, but after addition of RNF4 the oxyester underwent hydrolysis (Fig. 3a). The isolated RING domain of RNF4 was as efficient as the full-length protein in hydrolyzing the oxyester (Fig. 3b). The oxyester-linked ubiquitin was not transferred to lysine residues in RNF4, and formation of ubiquitin chains was not detected. Mass spectrometric analysis showed

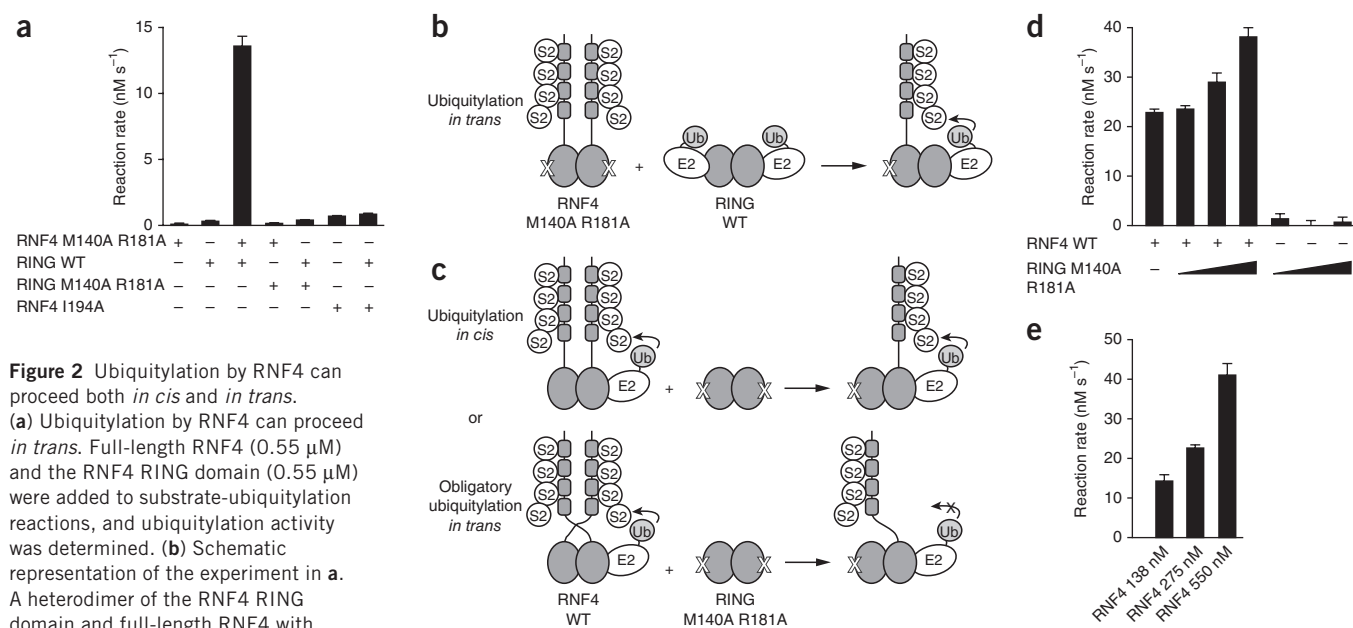


**Figure 2** Ubiquitylation by RNF4 can proceed both *in cis* and *in trans*.

(a) Ubiquitylation by RNF4 can proceed *in trans*. Full-length RNF4 (0.55  $\mu$ M) and the RNF4 RING domain (0.55  $\mu$ M) were added to substrate-ubiquitylation reactions, and ubiquitylation activity was determined. (b) Schematic representation of the experiment in a. A heterodimer of the RNF4 RING domain and full-length RNF4 with disrupted E2-binding site (M140A R181A) should be active in a substrate-ubiquitylation reaction provided ubiquitylation by RNF4 can proceed *in trans*. S2, SUMO-2.

(c) Schematic representation of a hypothesis behind the experiment in d. If ubiquitylation by RNF4 can proceed *in cis*, then a heterodimer of full-length RNF4 and the RNF4 RING domain with disrupted E2-binding site should have substrate-ubiquitylation activity. However, this heterodimer should be inactive if ubiquitylation can only proceed *in trans*. Therefore, addition of an excess of the RING domain with disrupted E2-binding site to wild-type RNF4 should result in inhibition of substrate-ubiquitylation activity provided ubiquitylation cannot proceed *in cis*. (d) Ubiquitylation by RNF4 can proceed *in cis*. The RING domain of RNF4 with disrupted E2-binding site (RING M140A R181A) was added to RNF4 WT (0.275  $\mu$ M) in 2-, 20- or 200-fold molar excess, and substrate-ubiquitylation activity was determined. (e) Under the conditions used in d, substrate-ubiquitylation activity is proportional to concentration of RNF4 in the reaction. In a,d,e, the data are mean  $\pm$  s.d. of duplicate reactions. Experiments were performed twice.

**Table 1** Data collection, phasing and refinement statistics

	SAD data set	Data set used for refinement
<b>Data collection</b>		
Space group	<i>P</i> 4 <sub>1</sub> 32	<i>P</i> 4 <sub>1</sub> 32
Cell dimensions		
<i>a</i> , <i>b</i> , <i>c</i> (Å)	72.6, 72.6, 72.6	72.6, 72.6, 72.6
Wavelength (Å)	1.28	0.98
Resolution (Å)	40.00–1.70 (1.76–1.70) <sup>a</sup>	18.00–1.50 (1.55–1.50)
<i>R</i> <sub>sym</sub>	0.079 (0.546)	0.062 (0.426)
<i>I</i> / $\sigma$ <i>I</i>	16.3 (4.4)	18.0 (2.9)
Completeness (%)	99.3 (100.0)	99.8 (100.0)
Redundancy	12.8 (13.0)	9.9 (7.3)
<b>Refinement</b>		
Resolution (Å)		18–1.5
No. reflections		10,391
<i>R</i> <sub>work</sub> / <i>R</i> <sub>free</sub>		0.168 / 0.197
No. atoms		
Protein		507
Zn <sup>2+</sup>		2
Sucrose/SO <sub>4</sub> <sup>2-</sup>		23/10
Water		54
<i>B</i> -factors		
Protein		24
Zn <sup>2+</sup>		20
Sucrose/SO <sub>4</sub> <sup>2-</sup>		25/46
Water		31
r.m.s. deviations		
Bond lengths (Å)		0.009
Bond angles (°)		1.44

<sup>a</sup>Values in parentheses are for highest-resolution shell. One crystal was used for each data set.

that a mixture of free ubiquitin (a product of hydrolysis) and ubiquitin linked to an amine group of a Tris molecule from the reaction buffer was released from the UbCH5a C85S~Ub oxyester after incubation with RNF4 (Supplementary Fig. 7). The oxyester was also cleaved by RNF4 in buffers lacking primary amine groups (MOPS and HEPES).

These results indicate that binding of the UbCH5a C85S~Ub oxyester to the RING domain of RNF4 activates the oxyester bond between ubiquitin and E2. We therefore asked whether dimerization of the RING domain has a role in the activation of the oxyester bond. Compared to wild-type RNF4, all the dimerization mutants were inefficient in hydrolyzing the UbCH5a C85S~Ub oxyester (Fig. 3b). Thus, the ability of the mutant proteins to cleave the UbCH5a C85S~Ub oxyester closely correlated with their substrate-ubiquitylation activities. Moreover, this assay uncouples RING-mediated activation of the bond connecting E2 and ubiquitin from transfer of ubiquitin to lysines.

Since neither the UbCH5a~Ub thioester nor the UbCH5a C85S~Ub oxyester is stable in the presence of RNF4, we generated a double mutant, UbCH5a N77A C85S, with the aim of producing a stable linkage between UbCH5a and ubiquitin. Asn77 is thought to stabilize the oxyanion intermediate formed when a lysine residue from the substrate attacks the E2~Ub thioester bond<sup>22</sup>. Indeed, UbCH5a N77A C85S~Ub was stable both in the absence and presence of RNF4 (Supplementary Fig. 8a). A mixture of UbCH5a N77A C85S, free ubiquitin and the E2~Ub oxyester was incubated with maltose-binding protein (MBP)-tagged RNF4 and bound proteins collected on amylose beads. Ubiquitin-charged UbCH5a was preferentially bound by RNF4 (Fig. 3c). Free UbCH5a interacted weakly, whereas binding of free ubiquitin could not be detected. Monomeric mutants of RNF4 (I192A and I194A) did not show this preferential

binding of E2~Ub, nor was any interaction observed with the E2 binding-deficient RNF4 M140A R181A.

Given that the UbCH5a~ubiquitin oxyester preferentially binds RNF4, the RING domain could have an additional interaction site for ubiquitin. Thus, the strict requirement for RING dimerization could be a consequence of UbCH5a binding to one monomer while the linked ubiquitin binds to the other monomer of RNF4. In a modeling program, we positioned the UbCH5~ubiquitin thioester onto the RING domain of RNF4, using the structure of UbCH5b bound to the RING of cIAP2 (ref. 18) to position the E2 on RNF4. A structure of the E2~Ub thioester was based on the structure of the UbCH5b~ubiquitin oxyester<sup>23</sup>. We generated the model manually by changing the position of ubiquitin relative to the E2 while retaining the thioester linkage. It is feasible to place ubiquitin across the dimer interface of the RING domain: this positions the E2 on one monomer in RNF4 while the linked ubiquitin reaches across the molecule and binds to residues at the dimer interface in the other monomer (Fig. 3d). In this model, the planar ring of Tyr193 of RNF4 engages the Ile44 hydrophobic patch of ubiquitin, centered on Ile44 and composed of Leu8, Val70 and Ile44. There are also potential contacts between the side chain of Leu152 of RNF4 and ubiquitin (Fig. 3e).

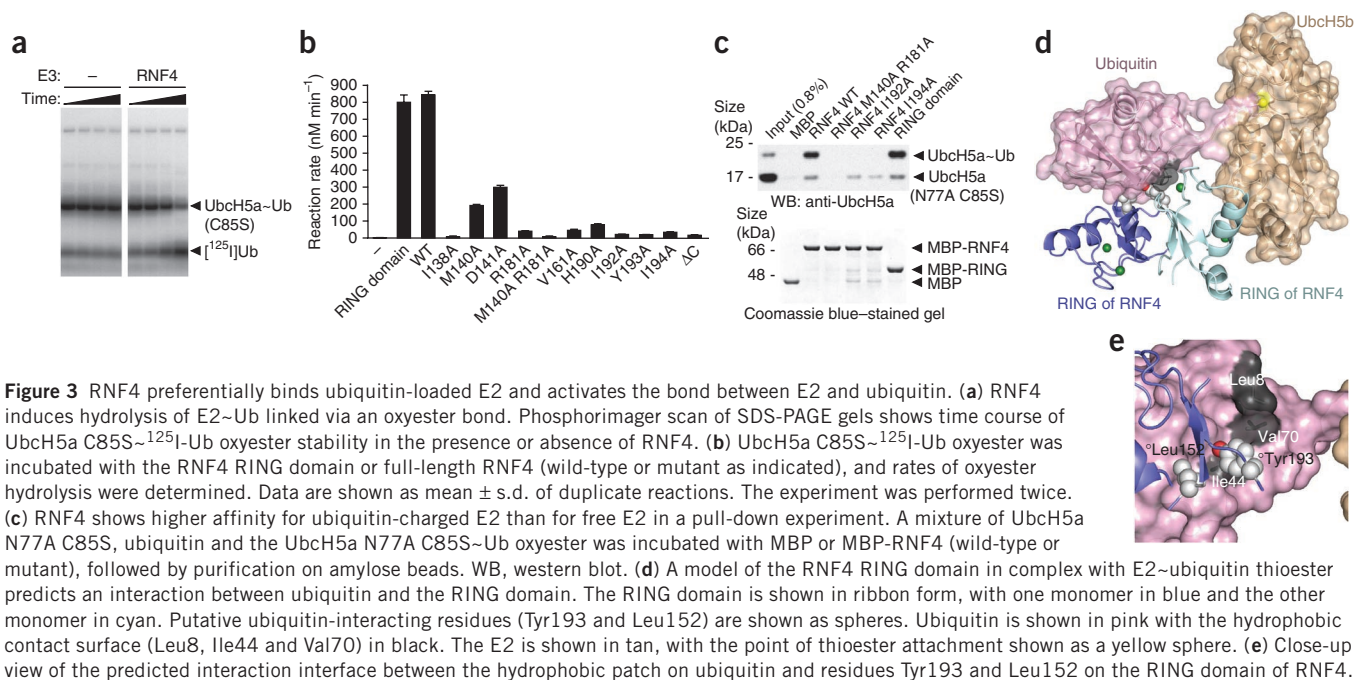
### Ile44 patch of ubiquitin is required for RNF4 activity

Most ubiquitin-binding domains interact with a solvent-exposed hydrophobic patch in ubiquitin that is centered on Ile44 and includes Leu8 and Val70 (ref. 24). Our model predicted this same surface was involved in recognition of the RNF4 RING domain. To test this, we used ubiquitin molecules in which the hydrophobic-patch interface was altered by mutagenesis (L8A, I44A and V70A). All ubiquitin mutants were efficiently loaded as thioesters onto UbCH5a (Fig. 4a). However, L8A and I44A were inactive in substrate ubiquitylation (with <0.5% the activity of wild-type ubiquitin), whereas V70A showed reduced activity (Fig. 4b). Mutation of other interaction sites on ubiquitin (F4A and D58A)<sup>25–27</sup> had no effect on substrate ubiquitylation. The intrinsic ability of UbCH5a charged with I44A ubiquitin to transfer the I44A ubiquitin to poly(L-lysine) in the absence of an E3 (ref. 28) showed a modest defect compared to UbCH5a loaded with wild-type ubiquitin (33% of wild-type activity) (Fig. 4c). However, this reduction in activity was small compared to the 200-fold difference in E3-dependent ubiquitylation activity. The oxyester bond between ubiquitin I44A and UbCH5a C85S was completely resistant to RNF4-mediated hydrolysis (Fig. 4d), and the conjugate between UbCH5a C85S and ubiquitin I44A did not interact with RNF4 (Fig. 4e). As expected, mutation of the E2-binding site in RNF4 M140A R181A abrogated binding to ubiquitin-loaded E2 (Fig. 4e). It should be noted that under the conditions used, binding of free E2 to RNF4 was not detected. Free E2 pulled down by wild-type RNF4 is a product of RNF4-mediated hydrolysis of the UbCH5a C85S~Ub oxyester (Supplementary Fig. 8b).

Thus, the Ile44 hydrophobic patch on ubiquitin is required for RNF4-mediated catalysis. However, this region also forms a noncovalent interaction with UbCH5 that influences processivity of ubiquitin addition<sup>23,29</sup>. This interaction is abolished by an S22R mutation in UbCH5 (ref. 29). Although substrate ubiquitylation with UbCH5a S22R was somewhat reduced, binding of UbCH5a S22R C85S~Ub oxyester to RNF4 and RNF4-induced hydrolysis of the oxyester was similar to wild-type (data not shown). Thus, the loss of activity seen with the Ile44-patch mutants of ubiquitin is not due to disruption of the noncovalent interaction between UbCH5a and ubiquitin.

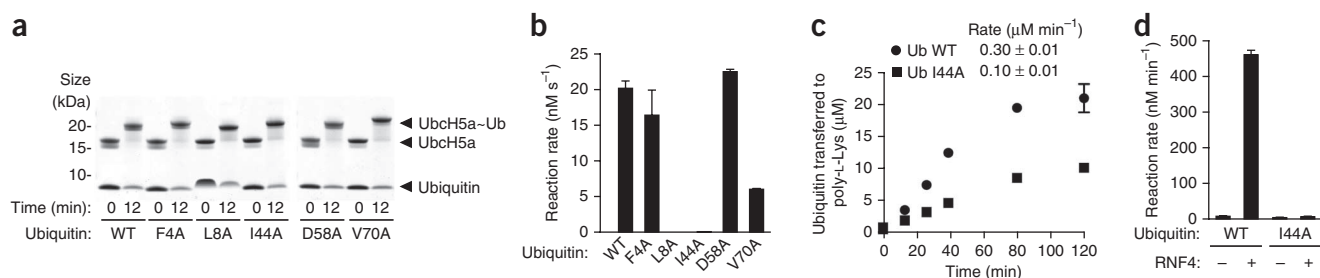
### Role of Tyr193 of RNF4 in E3 ligase activity

In the model of RNF4 bound to UbCH5 loaded with ubiquitin, the E2 binds to one monomer and ubiquitin reaches across the dimer



with the Ile44 hydrophobic patch engaging Tyr193 of the other RNF4 monomer (**Fig. 3d,e**). Tyr193 is required for dimerization, as the Y193A mutant is monomeric (**Supplementary Fig. 5**) and inactive as an E3 ligase (**Fig. 1e**). However, this residue is not buried in the dimer interface, but is surface exposed and appears to function by shielding the dimer interface (**Fig. 1d**). We therefore changed Tyr193 to histidine, reasoning that this mutant would retain the shielding function but, as the side chain of histidine is hydrophilic rather than hydrophobic, would be unable to interact with the hydrophobic

patch on ubiquitin. RNF4 Y193H (and Y193W) retained ability to dimerize, as assessed by gel-filtration chromatography, and its addition to a mixture of YFP-RING domain and ECFP-RNF4 led to a reduction in FRET signal. In contrast, monomeric RNF4 Y193A was unable to effect the reduction in FRET (**Fig. 5a**). As expected, the monomeric mutants were inactive in single-turnover substrate-ubiquitylation reactions. The Y193H mutant, although dimeric, was inactive, whereas Y193W (which retains hydrophobic character) had only a moderate reduction in ubiquitylation activity (**Fig. 5b**).



with the Ile44 hydrophobic patch engaging Tyr193 of the other RNF4 monomer (**Fig. 3d,e**). Tyr193 is required for dimerization, as the Y193A mutant is monomeric (**Supplementary Fig. 5**) and inactive as an E3 ligase (**Fig. 1e**). However, this residue is not buried in the dimer interface, but is surface exposed and appears to function by shielding the dimer interface (**Fig. 1d**). We therefore changed Tyr193 to histidine, reasoning that this mutant would retain the shielding function but, as the side chain of histidine is hydrophilic rather than hydrophobic, would be unable to interact with the hydrophobic

patch on ubiquitin. RNF4 Y193H (and Y193W) retained ability to dimerize, as assessed by gel-filtration chromatography, and its addition to a mixture of YFP-RING domain and ECFP-RNF4 led to a reduction in FRET signal. In contrast, monomeric RNF4 Y193A was unable to effect the reduction in FRET (**Fig. 5a**). As expected, the monomeric mutants were inactive in single-turnover substrate-ubiquitylation reactions. The Y193H mutant, although dimeric, was inactive, whereas Y193W (which retains hydrophobic character) had only a moderate reduction in ubiquitylation activity (**Fig. 5b**).

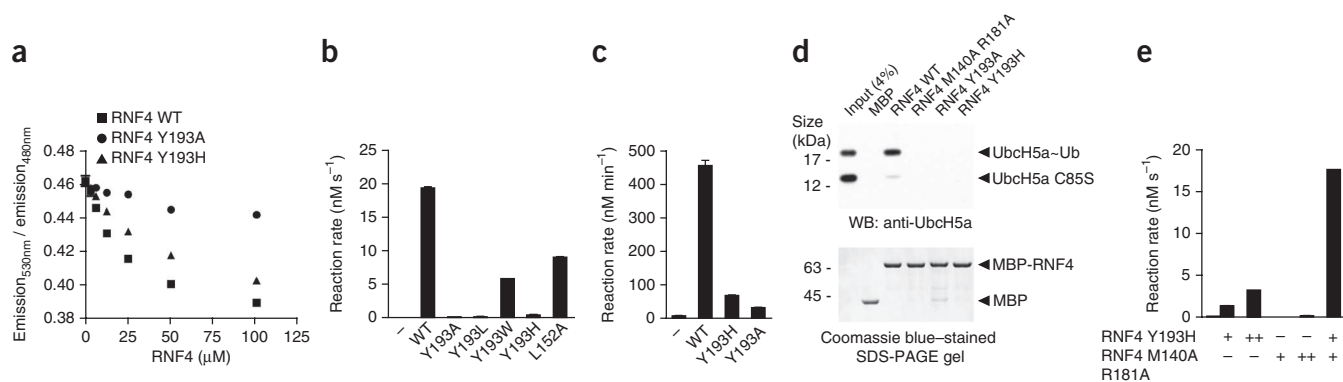
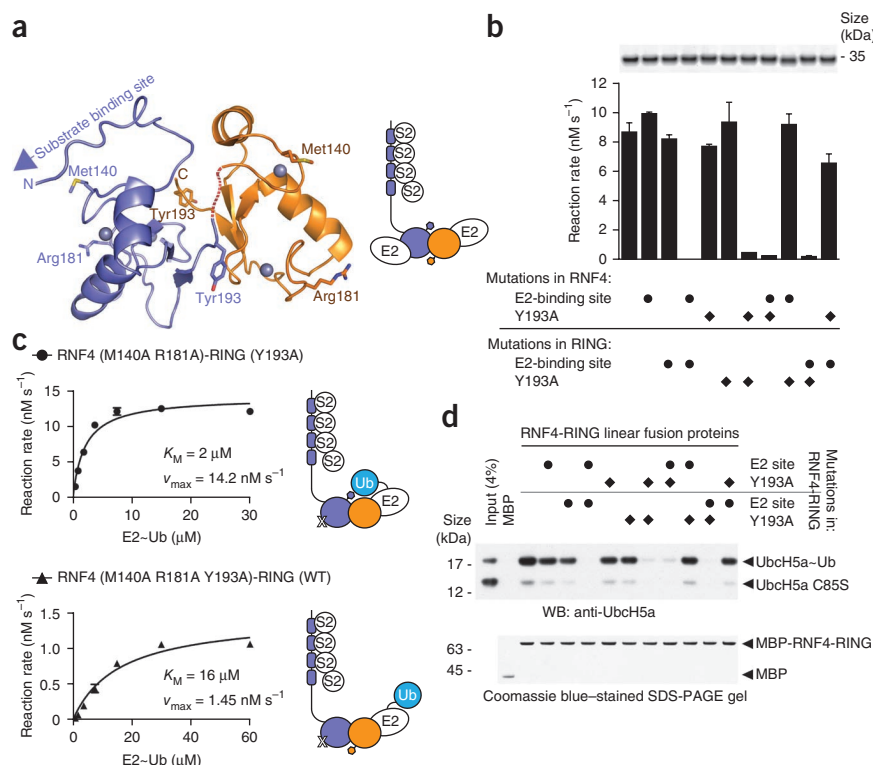


**Figure 5** Tyr193, a residue located at the dimer interface of the RNF4 RING domain, is required for activation of the thioester bond in the E2~ubiquitin thioester. **(a)** The ability of RNF4 Y193H to dimerize was assessed using a FRET-based dimerization assay. Unlabeled RNF4 was titrated into a mixture of ECFP-RNF4 and YFP-RING domain, and FRET signal was measured. Data points represent mean  $\pm$  s.d. of triplicate measurements. **(b)** Mutational analysis of the predicted ubiquitin-binding site on the RNF4 RING domain. Several mutations of Tyr193 were generated. Mutations to alanine and leucine disrupted RNF4 dimerization, but mutations to tryptophan and histidine did not. Substrate-ubiquitylation activity of the mutant proteins was determined using the single-turnover assay described in **Figure 1a**. **(c)** Tyr193 in RNF4 is required for efficient hydrolysis of the E2~ubiquitin oxyester. The Ubch5a C85S~Ub oxyester was incubated with RNF4 (wild-type or mutant as indicated) and the rate of oxyester hydrolysis was determined. **(d)** Mutation Y193H in RNF4 disrupts binding to the E2~ubiquitin oxyester. A pull-down experiment was performed as in **Figure 4e**. **(e)** Ubiquitylation activity of RNF4 Y193H can be rescued by addition of an inactive RNF4 mutant with disrupted E2-binding site (RNF4 M140A R181A). Substrate-ubiquitylation activity was determined as in **Figure 1a**. Final concentration of RNF4 mutants in the reaction was either 0.55  $\mu$ M (+) or 1.1  $\mu$ M (++) in **b,c,e**, data represent mean  $\pm$  s.d. of duplicate reactions. The experiments were performed twice.

Mutation of Leu152 in RNF4, which appears to contact ubiquitin in our model (the L152A mutant is also dimeric), resulted in a modest reduction in ubiquitylation activity (**Fig. 5b**). RNF4 Y193H was unable to efficiently catalyze hydrolysis of the Ubch5a C85S~Ub oxyester (**Fig. 5c**). Neither RNF4 Y193A nor RNF4 Y193H bound Ubch5a~ubiquitin (**Fig. 5d**). To rescue its ubiquitylation activity, the Y193H mutant of RNF4 was mixed with a mutant bearing a disrupted

E2-binding site (RNF4 M140A R181A). Although the individual molecules were inactive, the heterodimer showed substantial substrate-ubiquitylation activity (**Fig. 5e**). We infer that in the heterodimer, the E2 component of the E2~ubiquitin thioester binds to the Y193H subunit while the ubiquitin component of the E2~ubiquitin thioester engages Tyr193 of the M140A R181A subunit of RNF4, recreating a functional ubiquitin E3 ligase.

**Figure 6** A linear fusion of full-length RNF4 and the RNF4 RING domain shows that E2-binding site in one RING domain and Tyr193 in the other RING are both required for ubiquitylation activity. **(a)** A model of a linear fusion of full-length RNF4 and the RING domain of RNF4, based on the structure of the RNF4 RING domain reported here. A short linker between the C terminus of full-length RNF4 and the N terminus of the RING domain is shown as a red dashed line. Tyr193 at the dimer interface and residues important for E2 binding (Met140 and Arg181) are shown in stick representation. The linear fusion protein contains one substrate-binding site, two E2-binding sites and two Tyr193 residues, one on each side of the dimerization interface. A schematic representation of the RNF4-RING fusion protein is shown at right. **(b)** Substrate-ubiquitylation activity of RNF4-RING linear fusion proteins, with mutations in full-length RNF4 and/or the RNF4 RING domain. Data are shown as mean  $\pm$  s.d. of duplicate reactions. The experiment was performed twice. Top, SYPRO orange-stained SDS-PAGE gel with purified RNF4-RING fusion proteins (0.6  $\mu$ g). **(c)** Mutation of Tyr193 in the RING domain that does not bind E2 raises  $K_M$  and lowers  $k_{cat}$ . Michaelis-Menten kinetics were determined from reaction rates at various concentrations of Ubch5a~Ub thioester. **(d)** Binding of the E2~ubiquitin oxyester to RNF4-RING fusion proteins correlates well with their ubiquitylation activities. A pull-down experiment was performed as in **Figure 4e**.



As the RNF4 RING is in dynamic equilibrium between monomer and dimer and only the dimer is active, the concentration of dimer is crucial in evaluating the activity of RNF4. The homodimeric nature of RNF4 also means that it is not possible to introduce mutations into only one subunit of the dimer. To overcome these problems, we used a strategy previously employed for BRCA1–BARD1 (ref. 30) in which the two monomers are fused into a single polypeptide. The RNF4 RING crystal structure reveals that the C terminus of one RING is close to the N terminus of the other RING (Fig. 1c). We therefore fused the C terminus of full-length RNF4 to residue 131 at the N terminus of the RING domain to create the fusion protein containing a single substrate-binding site at the N terminus and two RING domains linked via a short spacer (Fig. 6a). Thus, mutations in the E2-binding site and Tyr193 can be asymmetrically introduced into the fusion protein. Consistent with our model, mutation of the E2-binding site (M140A R181A) in only one RING did not affect substrate-ubiquitylation activity (Fig. 6b). Likewise, introduction of the Y193A mutation into one RING was without consequence; however, introduction of the E2-binding site mutations or the Y193A mutation into both RINGs markedly reduced ubiquitylation activity (Fig. 6b). Combining the E2-binding site mutations with the Y193A mutation in the same RING abrogated E3 ligase activity, whereas introducing the E2-binding site mutations into one RING and the Y193A mutation into the other RING yielded wild-type activity (Fig. 6b). These data confirm the requirement for the E2-binding site and Tyr193 to be present on opposite subunits of the RNF4 dimer.

To establish the role of Tyr193 in ubiquitin transfer, we carried out Michaelis-Menten analysis of substrate ubiquitylation, comparing fusion proteins that have E2-binding site mutations and the Y193A mutation in the same RING or in different RINGs. With 4× SUMO-2 substrate in excess, initial rate measurements of substrate ubiquitylation were collected at a range of concentrations of ubiquitin-loaded E2. The RNF4-RING fusion with E2-binding site mutations and Y193A mutation in different RINGs, which showed wild-type activity, had a lower  $K_M$  for ubiquitin-loaded UbcH5a (2  $\mu\text{M}$  compared to 16  $\mu\text{M}$ ) and a higher  $v_{\text{max}}$  (14.2  $\text{nM s}^{-1}$  compared to 1.45  $\text{nM s}^{-1}$ ) than the otherwise identical fusion construct with the E2-binding site mutations and Y193A mutation in the same RING (Fig. 6c). This suggests that ubiquitin-loaded E2 has a higher affinity for the RING dimer when it can engage the Tyr193 residue from the RING subunit that does not interact with E2. However, the data also indicate that engagement of Tyr193 in the RING by ubiquitin-loaded E2 has a direct effect on catalysis. Consistent with the effect on  $K_M$ , the RNF4-RING fusion proteins with E2-binding site mutations and Y193A mutation in the same RING did not efficiently bind ubiquitin-loaded E2, whereas versions of RNF4-RING with these mutations in opposite RINGs showed selective binding of ubiquitin-loaded E2 (Fig. 6d).

## DISCUSSION

Dimeric RING ubiquitin ligases are modular proteins containing a substrate-binding domain and a RING domain that is the catalytic engine of ubiquitylation. This is exemplified by RNF4, in which the N-terminal domain binds to the poly-SUMO substrate, whereas the RING domain is responsible for ubiquitin transfer. RING dimerization is essential for ubiquitin E3 ligase activity of RNF4, but a mechanistic understanding of this requirement has remained elusive<sup>17</sup>. Modeling suggested that UbcH5 could bind to one monomer of RNF4 while the thioester-linked ubiquitin reached across the molecule to contact the other monomer of the dimer. In this model, the hydrophobic patch centered on Ile44 of ubiquitin engages the conserved Tyr193 located at the dimer interface. Mutation of residues in the hydrophobic patch

of ubiquitin abrogated RING-dependent transfer of ubiquitin to substrate, preferential binding of ubiquitin-loaded E2 to the RING, and RING-dependent activation of the E2~ubiquitin bond. RNF4 Y193H, although dimeric, was inactive and unable to preferentially bind ubiquitin-loaded UbcH5a, consistent with the requirement for a hydrophobic residue to engage the Ile44 patch. The other crucial interface was between UbcH5a and the RING: mutations in the RING that disrupted this interaction resulted in an inactive E3 ligase and abolished binding of ubiquitin-loaded E2.

Creation of a fusion between the two RINGs of RNF4 allowed us to directly test the requirement for the E2-binding site and Tyr193 within the context of the dimer. Mutating these sites in the same RING markedly reduced ubiquitylation, whereas a dimer with these mutations in opposite RINGs had wild-type activity. Michaelis-Menten analysis revealed that the lower activity in the former mutant was due to a higher  $K_M$  for ubiquitin-loaded E2 and a lower  $v_{\text{max}}$  for ubiquitin transfer to substrate. These data, together with our direct binding data, suggest that an E2-binding site in one RING and Tyr193 in the other RING are both required to recruit the ubiquitin-loaded E2. Presumably, this interaction alters the conformation of the active site of the E2, facilitating ubiquitin transfer to a lysine residue in substrate. This is consistent with our data, which indicate that binding of both E2 and ubiquitin to RNF4 causes activation of the thioester bond in E2~Ub. Once isopeptide bond formation has taken place, the weak binding of free E2 and ubiquitin would favor their dissociation and facilitate rapid rebinding of ubiquitin-charged E2, required for processive synthesis of ubiquitin chains<sup>31,32</sup>.

Homo- or heterodimerization has been observed for a number of RING-type ubiquitin E3 ligases, including cIAP2 (ref. 18), TRAF6 (ref. 21), MDM2–MDMX<sup>19</sup>, BRCA1–BARD1 (ref. 33) and Ring1b–Bmi1 (ref. 34), and also for structurally related U-box ubiquitin E3 ligases Prp19 (ref. 20) and CHIP<sup>35,36</sup>. Even though the structural elements that form dimerization interfaces in these dimers vary, the relative orientation of the two RING or U-box domains is similar. As dimerization is necessary for ubiquitylation activity, this suggests similar catalytic mechanism for these dimeric ubiquitin E3 ligases.

Our results indicate that the RING domain of RNF4 contacts both E2 and ubiquitin upon binding to the E2~Ub thioester. A similar finding has recently been reported for the HECT-type ubiquitin E3 ligase NEDD4L; a structure of this ligase with UbcH5b~Ub reveals that extensive noncovalent interactions between ubiquitin and the HECT domain are required for proper positioning of the E2 and E3 active sites<sup>37</sup>. An interesting interaction has also been observed between UbcH5~Ub and SspH2, an atypical bacterial ubiquitin E3 ligase<sup>38</sup>. SspH2 has no detectable affinity for free UbcH5, but binds to ubiquitin-charged UbcH5, recognizing regions on both E2 and ubiquitin<sup>38</sup>. Although these E3 ligases are mechanistically very different, noncovalent interactions between ubiquitin and E3 might be a common theme in E3-catalyzed ubiquitylation reactions.

In our model, the ubiquitin linked to the E2 is in an extended conformation that is based on the structure of a UbcH5b~ubiquitin oxyster<sup>23</sup>, in which the Ile44 hydrophobic patch of ubiquitin engages in a ‘backside’ interaction with UbcH5b. While this backside interaction may be important for processive ubiquitin addition, it is not required for substrate ubiquitylation mediated by RNF4, as an S22R mutation in UbcH5a had a much smaller effect on substrate ubiquitylation than mutations of the Ile44 patch in ubiquitin. Even in the absence of this backside interaction, the UbcH5a~ubiquitin is likely to be in an extended conformation, as this has been observed by NMR for the UbcH5c S22R C85S~ubiquitin conjugate<sup>39</sup>. Recent studies on K11 chain synthesis by Ube2S have suggested that the donor

ubiquitin also makes noncovalent contacts via the Ile44 hydrophobic patch with the E2 to which it is thioester-linked<sup>40</sup>. This interaction has also been shown to be important in enabling ubiquitin to act as a donor for chain initiation or elongation by ubiquitin-loaded Cdc34 (ref. 41). Although I44A ubiquitin had a reduced inherent ability to be transferred from E2 to substrate in the absence of an E3 (Fig. 4c), this effect was rather modest (activity 33% that of wild type) and is unlikely to account for the large E3-dependent effect (activity <0.5% of wild type) that we observed with this mutant (Fig. 4b).

RING-domain ubiquitin E3 ligases are often viewed as scaffold proteins that bring ubiquitin-charged E2 and a substrate into close proximity and thus facilitate transfer of ubiquitin from E2 to the substrate. However, our data indicate that dimeric RING-type ubiquitin E3 ligases have a more active role, facilitating catalysis by binding both E2 and ubiquitin and thus activating the E2~Ub thioester bond.

## METHODS

Methods and any associated references are available in the online version of the paper at <http://www.nature.com/nsmb/>.

**Accession codes.** Protein Data Bank: Coordinates and structure factors for the RING domain of RNF4 have been deposited under accession code 2XEU.

*Note: Supplementary information is available on the Nature Structural & Molecular Biology website.*

## ACKNOWLEDGMENTS

We thank C. Botting for mass spectrometric analysis, M. Agacan for analytical ultracentrifugation analysis and N. Wood for help with cloning. His-Ube1 was a kind gift from the Division of Signal Transduction Therapy, University of Dundee. The sequence encoding RNF4 ΔC in pLou3 vector was a kind gift from L. Shen, University of Dundee. A.P. was funded by a studentship from the Wellcome Trust. This work was supported by a grant to R.T.H. from Cancer Research UK. The structural biology was supported by the Scottish Funding Council (reference SULSA) and by the UK Biotechnology and Biological Sciences Research Council through the SPoRT initiative.

## AUTHOR CONTRIBUTIONS

A.P. purified RNF4 proteins, carried out crystallography, conducted biochemical analysis and interpreted the data. E.G.J. purified recombinant proteins and carried out ubiquitylation assays. S.A.M., K.A.J. and J.H.N. contributed to structural analysis. I.N. contributed to biochemical analysis. A.P., J.H.N. and R.T.H. wrote the paper. R.T.H. conceived the project and contributed to data interpretation.

## COMPETING FINANCIAL INTERESTS

The authors declare no competing financial interests.

Published online at <http://www.nature.com/nsmb/>.

Reprints and permissions information is available online at <http://www.nature.com/reprints/index.html>.

- Dye, B.T. & Schulman, B.A. Structural mechanisms underlying posttranslational modification by ubiquitin-like proteins. *Annu. Rev. Biophys. Biomol. Struct.* **36**, 131–150 (2007).
- Pickart, C.M. & Eddins, M.J. Ubiquitin: structures, functions, mechanisms. *Biochim. Biophys. Acta* **1695**, 55–72 (2004).
- Deshaies, R.J. & Joazeiro, C.A. RING domain E3 ubiquitin ligases. *Annu. Rev. Biochem.* **78**, 399–434 (2009).
- Hay, R.T. SUMO: a history of modification. *Mol. Cell* **18**, 1–12 (2005).
- Perry, J.J., Tainer, J.A. & Boddy, M.N. A SIM-ultaneous role for SUMO and ubiquitin. *Trends Biochem. Sci.* **33**, 201–208 (2008).
- Kosoy, A., Calonge, T.M., Outwin, E.A. & O'Connell, M.J. Fission yeast Rnf4 homologs are required for DNA repair. *J. Biol. Chem.* **282**, 20388–20394 (2007).
- Prudden, J. *et al.* SUMO-targeted ubiquitin ligases in genome stability. *EMBO J.* **26**, 4089–4101 (2007).
- Sun, H., Levenson, J.D. & Hunter, T. Conserved function of RNF4 family proteins in eukaryotes: targeting a ubiquitin ligase to SUMOylated proteins. *EMBO J.* **26**, 4102–4112 (2007).
- Uzunova, K. *et al.* Ubiquitin-dependent proteolytic control of SUMO conjugates. *J. Biol. Chem.* **282**, 34167–34175 (2007).
- Xie, Y. *et al.* The yeast Hex3.Slx8 heterodimer is a ubiquitin ligase stimulated by substrate sumoylation. *J. Biol. Chem.* **282**, 34176–34184 (2007).
- Häkli, M., Loric, K.L., Weissman, A.M., Janne, O.A. & Palvimo, J.J. Transcriptional coregulator SNURF (RNF4) possesses ubiquitin E3 ligase activity. *FEBS Lett.* **560**, 56–62 (2004).
- Lallemant-Breitenbach, V. *et al.* Arsenic degrades PML or PML-RAR $\alpha$  through a SUMO-triggered RNF4/ubiquitin-mediated pathway. *Nat. Cell Biol.* **10**, 547–555 (2008).
- Tatham, M.H. *et al.* RNF4 is a poly-SUMO-specific E3 ubiquitin ligase required for arsenic-induced PML degradation. *Nat. Cell Biol.* **10**, 538–546 (2008).
- Song, J., Durrin, L.K., Wilkinson, T.A., Krontiris, T.G. & Chen, Y. Identification of a SUMO-binding motif that recognizes SUMO-modified proteins. *Proc. Natl. Acad. Sci. USA* **101**, 14373–14378 (2004).
- Hecker, C.M., Rabiller, M., Haglund, K., Bayer, P. & Dikic, I. Specification of SUMO1- and SUMO2-interacting motifs. *J. Biol. Chem.* **281**, 16117–16127 (2006).
- Song, J., Zhang, Z., Hu, W. & Chen, Y. Small ubiquitin-like modifier (SUMO) recognition of a SUMO binding motif: a reversal of the bound orientation. *J. Biol. Chem.* **280**, 40122–40129 (2005).
- Liew, C.W., Sun, H., Hunter, T. & Day, C.L. RING domain dimerization is essential for RNF4 function. *Biochem. J.* **431**, 23–29 (2010).
- Mace, P.D. *et al.* Structures of the cIAP2 RING domain reveal conformational changes associated with ubiquitin-conjugating enzyme (E2) recruitment. *J. Biol. Chem.* **283**, 31633–31640 (2008).
- Linke, K. *et al.* Structure of the MDM2/MDMX RING domain heterodimer reveals dimerization is required for their ubiquitylation in trans. *Cell Death Differ.* **15**, 841–848 (2008).
- Vander Kooi, C.W. *et al.* The Prp19 U-box crystal structure suggests a common dimeric architecture for a class of oligomeric E3 ubiquitin ligases. *Biochemistry* **45**, 121–130 (2006).
- Yin, Q. *et al.* E2 interaction and dimerization in the crystal structure of TRAF6. *Nat. Struct. Mol. Biol.* **16**, 658–666 (2009).
- Wu, P.Y. *et al.* A conserved catalytic residue in the ubiquitin-conjugating enzyme family. *EMBO J.* **22**, 5241–5250 (2003).
- Sakata, E. *et al.* Crystal structure of UbcH5b-ubiquitin intermediate: insight into the formation of the self-assembled E2~Ub conjugates. *Structure* **18**, 138–147 (2010).
- Dikic, I., Wakatsuki, S. & Walters, K.J. Ubiquitin-binding domains—from structures to functions. *Nat. Rev. Mol. Cell Biol.* **10**, 659–671 (2009).
- Lee, S. *et al.* Structural basis for ubiquitin recognition and autoubiquitination by Rabex-5. *Nat. Struct. Mol. Biol.* **13**, 264–271 (2006).
- Penengo, L. *et al.* Crystal structure of the ubiquitin binding domains of rabex-5 reveals two modes of interaction with ubiquitin. *Cell* **124**, 1183–1195 (2006).
- Rahighi, S. *et al.* Specific recognition of linear ubiquitin chains by NEMO is important for NF- $\kappa$ B activation. *Cell* **136**, 1098–1109 (2009).
- Mastrandrea, L.D., Kasperek, E.M., Niles, E.G. & Pickart, C.M. Core domain mutation (S86Y) selectively inactivates polyubiquitin chain synthesis catalyzed by E2~25K. *Biochemistry* **37**, 9784–9792 (1998).
- Brzovic, P.S., Lissounov, A., Christensen, D.E., Hoyt, D.W. & Kleivit, R.E.A. UbcH5/ubiquitin noncovalent complex is required for processive BRCA1-directed ubiquitination. *Mol. Cell* **21**, 873–880 (2006).
- Christensen, D.E., Brzovic, P.S. & Kleivit, R.E. E2-BRCA1 RING interactions dictate synthesis of mono- or specific polyubiquitin chain linkages. *Nat. Struct. Mol. Biol.* **14**, 941–948 (2007).
- Kleiger, G., Saha, A., Lewis, S., Kuhlman, B. & Deshaies, R.J. Rapid E2~E3 assembly and disassembly enable processive ubiquitylation of cullin-RING ubiquitin ligase substrates. *Cell* **139**, 957–968 (2009).
- Pierce, N.W., Kleiger, G., Shan, S.O. & Deshaies, R.J. Detection of sequential polyubiquitylation on a millisecond timescale. *Nature* **462**, 615–619 (2009).
- Brzovic, P.S., Rajagopal, P., Hoyt, D.W., King, M.C. & Kleivit, R.E. Structure of a BRCA1-BARD1 heterodimeric RING-RING complex. *Nat. Struct. Biol.* **8**, 833–837 (2001).
- Buchwald, G. *et al.* Structure and E3-ligase activity of the Ring-Ring complex of Polycomb proteins Bmi1 and Ring1b. *EMBO J.* **25**, 2465–2474 (2006).
- Xu, Z. *et al.* Interactions between the quality control ubiquitin ligase CHIP and ubiquitin conjugating enzymes. *BMC Struct. Biol.* **8**, 26 (2008).
- Zhang, M. *et al.* Chaperoned ubiquitylation—crystal structures of the CHIP U box E3 ubiquitin ligase and a CHIP-Ubc13-Uev1a complex. *Mol. Cell* **20**, 525–538 (2005).
- Kamadurai, H.B. *et al.* Insights into ubiquitin transfer cascades from a structure of a UbcH5B-ubiquitin-HECT(NEDD4L) complex. *Mol. Cell* **36**, 1095–1102 (2009).
- Levin, I. *et al.* Identification of an unconventional E3 binding surface on the UbcH5~Ub conjugate recognized by a pathogenic bacterial E3 ligase. *Proc. Natl. Acad. Sci. USA* **107**, 2848–2853 (2010).
- Pruneda, J.N., Stoll, K.E., Bolton, L.J., Brzovic, P.S. & Kleivit, R.E. Ubiquitin in motion: structural studies of the ubiquitin-conjugating enzyme-ubiquitin conjugate. *Biochemistry* **50**, 1624–1633 (2011).
- Wickliffe, K.E., Lorenz, S., Wemmer, D.E., Kuriyan, J. & Rape, M. The mechanism of linkage-specific ubiquitin chain elongation by a single-subunit E2. *Cell* **144**, 769–781 (2011).
- Saha, A., Lewis, S., Kleiger, G., Kuhlman, B. & Deshaies, R.J. Essential role for ubiquitin-ubiquitin-conjugating enzyme interaction in ubiquitin discharge from Cdc34 to substrate. *Mol. Cell* **42**, 75–83 (2011).

## ONLINE METHODS

**cDNA constructs.** Constructs for full-length *Rattus norvegicus* RNF4 (wild-type RNF4) and RNF4 mtSIM1,2,3,4 (SIMs mutant) have been described previously<sup>13</sup>. Sequences encoding the RING domain of RNF4 (residues 134–194), RNF4<sub>32–76</sub> (residues 32–76) and RNF4<sub>32–133</sub> (residues 32–133) were subcloned into pLou3 vector<sup>13</sup> and as a result of cloning, these constructs contain three extra residues (Gly-Ala-Met) after the TEV protease cleavage site. Sequence encoding RNF4  $\Delta$ C (residues 1–190) in pLou3 vector was a kind gift from L. Shen, University of Dundee. To generate a linear fusion of full-length RNF4 and the RING domain of RNF4 (termed RNF4-RING), full-length RNF4 sequence was subcloned into pLou3 vector using NcoI and BamHI restriction sites and the RNF4 RING domain (residues 131–194) was inserted using BamHI and HindIII sites. There is a single glycine residue as a linker between RNF4 and the RNF4 RING domain. For FRET-based assays, sequences for RNF4 and the RING domain of RNF4 were subcloned into pHIS-TEV-ECFP and pHIS-TEV-Venus-YFP plasmids<sup>42</sup>. Sequence encoding 4 $\times$  SUMO-2, a linear head-to-tail fusion of four SUMO-2 molecules, was subcloned into pHIS-TEV-30a vector<sup>43</sup>. All SUMO-2s in the fusion protein have the first methionine changed to glycine. Details of cloning are available upon request. Human UbcH5a was subcloned into pHIS-TEV-30a vector. Point mutations were introduced using the QuikChange site-directed mutagenesis kit (Stratagene).

**Protein expression and purification.** Proteins were expressed in bacteria and purified by standard methods. Detailed protocols are in **Supplementary Methods**.

**Crystallization and structure determination.** Crystals of the RING domain of RNF4 were grown using the sitting-drop vapor diffusion method at 20 °C. We mixed 1  $\mu$ l of the RNF4 RING domain (5.5 mg ml<sup>-1</sup> in 20 mM Tris, 150 mM NaCl, 1 mM TCEP pH 7.0) with 1  $\mu$ l of reservoir solution (2M (NH<sub>4</sub>)<sub>2</sub>SO<sub>4</sub>, 200 mM NaCl, 100 mM sodium cacodylate pH 7.0) and 0.2  $\mu$ l of 30% (w/v) sucrose. Crystals grew to their final size of ~0.15 mm  $\times$  0.15 mm  $\times$  0.15 mm in 2–3 d. Before flash-freezing in liquid nitrogen, crystals were briefly soaked in a cryoprotectant solution (15:85 (v/v) reservoir solution and saturated solution of sucrose in the reservoir solution).

Diffraction data were collected at 100 K at beamline ID14-4 at the European Synchrotron Radiation Facility, Grenoble, France. The structure was solved by SAD using the anomalous signal from the two zinc ions bound to the RING domain. A SAD data set was collected at the zinc-absorption peak wavelength (1.28 Å, determined by fluorescence scan). A second data set for refinement from a different crystal was collected at a wavelength of 0.98 Å. All diffraction data were processed using HKL2000 (ref. 44). Phases were obtained using SHELXC/D/E<sup>45</sup> and an initial model was built by ARP/wARP<sup>46</sup>. This model was refined using REFMAC5 (ref. 47) from the CCP4 suite<sup>48</sup>, followed by iterative cycles of manual rebuilding using Coot<sup>49</sup> and further refinement. Translation, libration and screw rotation (TLS) parameters were used in the final cycles of refinement<sup>50</sup>. Data collection and refinement statistics are shown in **Table 1**. The geometry of the final model was checked with MolProbity<sup>51</sup>. There were 98.4% of residues in the favored region of the Ramachandran plot, with the remaining 1.6% being in the allowed region. The dimerization interface of RNF4 was analyzed using the PISA server at the European Bioinformatics Institute<sup>52</sup>. Structural representations and models were generated using PyMol (Schrödinger).

**Single-turnover substrate-ubiquitylation assay.** E2 (UbcH5a) was first charged with ubiquitin in the absence of an E3 and a substrate. To prepare the UbcH5a~Ub thioester, we incubated UbcH5a and ubiquitin (both 100  $\mu$ M) with 0.2  $\mu$ M Ube1 in 50 mM Tris, 150 mM NaCl, 3 mM ATP, 5 mM MgCl<sub>2</sub>, 0.5 mM TCEP and 0.1% (v/v) NP40 (pH 7.5) at 37 °C for 12 min. To stop E1-mediated loading of E2 with ubiquitin, we depleted ATP by adding apyrase (4.5 U ml<sup>-1</sup>; New England BioLabs) and incubating the reaction at room temperature for 10 min. Efficiency of UbcH5a~Ub thioester formation was estimated to be approximately 60%. <sup>125</sup>I-labeled 4 $\times$  SUMO-2 (~750 Ci mol<sup>-1</sup>) was used as a substrate for RNF4-mediated ubiquitylation. The UbcH5a~Ub thioester (~20  $\mu$ M) was incubated with RNF4 (0.275  $\mu$ M unless specified otherwise in figure legends) and <sup>125</sup>I-4 $\times$  SUMO-2 (5.5  $\mu$ M) at room temperature. Reactions were stopped by addition of reducing SDS-PAGE loading buffer and analyzed by SDS-PAGE followed by phosphorimaging. Percentage of substrate modified with ubiquitin was determined by quantification of phosphorimager scans using AIDA software (Raytest). Reaction time points were taken from 30 s to up to 20 min, and reaction rates were determined using at least three time points within the linear range of the reaction. Reactions were carried out in duplicate and reaction rates are shown as mean  $\pm$  s.d. Examples of primary data are shown in **Supplementary Figure 9**.

Substrate-ubiquitylation reactions with RNF4-RING linear fusion proteins as E3 contained ~20  $\mu$ M UbcH5a~Ub thioester, 5.5  $\mu$ M <sup>125</sup>I-4 $\times$  SUMO-2 and 35 nM RNF4-RING fusion protein. To determine Michaelis-Menten kinetics, initial rate measurements of substrate ubiquitylation were collected at a range of concentrations of the UbcH5a~Ub thioester (0.5–60  $\mu$ M). Reaction time points were taken from 1 min to up to 4 min for RNF4 M140A R181A-RING Y193A, and from 15 min to up to 2 h for RNF4 M140A R181A Y193A-RING WT. Reaction rates were determined using three time points within the linear range of the reaction. Data were analyzed using GraphPad Prism (GraphPad Software).

**Other biochemical assays.** Detailed procedures are described in **Supplementary Methods**.

42. Martin, S.F., Tatham, M.H., Hay, R.T. & Samuel, I.D. Quantitative analysis of multi-protein interactions using FRET: application to the SUMO pathway. *Protein Sci.* **17**, 777–784 (2008).
43. Martin, S.F., Hattersley, N., Samuel, I.D., Hay, R.T. & Tatham, M.H. A fluorescence-resonance-energy-transfer-based protease activity assay and its use to monitor paralog-specific small ubiquitin-like modifier processing. *Anal. Biochem.* **363**, 83–90 (2007).
44. Otwinowski, Z. & Minor, W. Processing of X-ray diffraction data collected in oscillation mode. *Methods Enzymol.* **276**, 307–326 (1997).
45. Sheldrick, G.M. A short history of SHELX. *Acta Crystallogr. A* **64**, 112–122 (2008).
46. Morris, R.J., Perrakis, A. & Lamzin, V.S. ARP/wARP and automatic interpretation of protein electron density maps. *Methods Enzymol.* **374**, 229–244 (2003).
47. Murshudov, G.N., Vagin, A.A. & Dodson, E.J. Refinement of macromolecular structures by the maximum-likelihood method. *Acta Crystallogr. D Biol. Crystallogr.* **53**, 240–255 (1997).
48. Winn, M.D. *et al.* Overview of the CCP4 suite and current developments. *Acta Crystallogr. D Biol. Crystallogr.* **67**, 235–242 (2011).
49. Emsley, P., Lohkamp, B., Scott, W.G. & Cowtan, K. Features and development of Coot. *Acta Crystallogr. D Biol. Crystallogr.* **66**, 486–501 (2010).
50. Winn, M.D., Isupov, M.N. & Murshudov, G.N. Use of TLS parameters to model anisotropic displacements in macromolecular refinement. *Acta Crystallogr. D Biol. Crystallogr.* **57**, 122–133 (2001).
51. Davis, I.W. *et al.* MolProbity: all-atom contacts and structure validation for proteins and nucleic acids. *Nucleic Acids Res.* **35**, W375–83 (2007).
52. Krissinel, E. & Henrick, K. Inference of macromolecular assemblies from crystalline state. *J. Mol. Biol.* **372**, 774–797 (2007).